



# Linking processing to formulation in dynamic membranes of tunable pore size for lemon oil emulsions

W. Kaade, M. Ferrando, S. de Lamo-Castellví, C. Güell \*

Departament d'Enginyeria Química, Universitat Rovira i Virgili, Avda. Països Catalans 26, 43007, Tarragona, Spain

## ARTICLE INFO

### Keywords:

Lemon oil  
Encapsulation  
Whey protein  
Sodium caseinate  
Carboxymethyl cellulose electrostatic complex  
Membrane emulsification

## ABSTRACT

Lemon oil is widely used for food flavoring purposes, but due to its low water solubility and tendency to oxidation, requires encapsulation in oil-in-water (O/W) emulsions. Therefore, this study assesses the use of two natural biopolymers and a tailor-made one to encapsulate lemon oil with a dynamic membrane of tunable pore size (DMTS). This emulsification system, consisting of an outer bed layer of silica beads sitting upon a metal microporous metallic membrane, overcomes the limitations of conventional emulsification membranes, such as low throughput, complex cleaning before reuse, fixed membrane thickness and pore size, and significative protein fouling. The effects of the DMTS characteristics on the droplet size distribution and emulsion productivity were studied. The results demonstrate that mono-dispersed emulsions can be obtained using dynamic membranes for all the biopolymers studied and the productivity can reach  $1000 \text{ m}^3 \text{ m}^{-2} \text{ h}^{-1}$  pointing out the suitability of this system for scale-up.

## 1. Introduction

Food emulsions have been used for the encapsulation of flavors, antioxidants, and other active ingredients. However, what is necessary for food emulsions, in general, is for them to remain stable that is to maintain their physicochemical properties over time. One of the main features essential to lengthen emulsion stability is the presence of small and monodispersed droplets. To achieve this aim, energy-intensive techniques like rotor-stator systems, high-pressure homogenizers, or colloid mills have been used traditionally (Bai et al., 2017; Rao and McClements, 2012a). These methods, however, are not the best suited to produce emulsions encapsulating heat and shear sensitive ingredients, such as food aromas and proteins, respectively. Hence, membrane emulsification (ME) has served as a low shear replacement for the production of food emulsions (Joscelyne and Trägårdh, 1999; Kandori, 1995; Wang et al., 2020), since with ME devices, the production of monodispersed emulsions at low shear conditions and a minimum increase of working temperatures is possible (Dragosavac et al., 2012).

One particular system of ME that is reported in the literature is referred to as a dynamic membranes (Nazir and Vladisavljević, 2021; Van Der Zwan et al., 2008). It is a microporous system that consists of a porous bed/layer of silica glass micro-beads supported by a porous nickel micro-sieve. This system is reported to yield high throughput

( $\approx 1000 \text{ m}^3 \text{ m}^{-2} \text{ h}^{-1}$ ), produce monodispersed emulsions, and be easy to clean and re-use (Nazir et al., 2013). A number of studies have used this system to produce food-grade emulsions. Sunflower oil-in-water emulsions (Eisinaite et al., 2016; Ladjal Ettoumi et al., 2017),  $W_1/O/W_2$  double (Sahin et al., 2014; Wang et al., 2020) emulsions, and food foams (Nazir et al., 2015) were reported in the literature to be produced with dynamic membranes. Dynamic membranes of tunable pore size (DMTS) have also been used to produce food-grade O/W emulsions encapsulating lemon oil (up to 40 %wt), stabilized by a small molecular weight surfactant, polyoxyethylene sorbitan monolaurate (Tween 20) (Kaade et al., 2020). The DMTS system has been shown effective in the ease of tuning the emulsions' droplet sizes by controlling the micro-beads size and bed height. Besides, due to the nature of Tween 20, there was no noticeable fouling during the emulsification process. Wang et al. (2021b) also used the DMTS system to stabilize sunflower oil in water emulsions with whey protein (WP) however a connection between the DMTS process parameters and the formulation results is yet to be made.

The effective encapsulation of lemon oil, which often requires a final spray-drying step, can benefit from the use of biopolymers such as milk proteins or protein-polysaccharide complexes that will enhance the protection of the active ingredients during processing. This study assesses the performance of dynamic microporous membranes to encapsulate lemon oil stabilized with a tailor-made biopolymer (whey protein-

\* Corresponding author.

E-mail address: [carme.guell@urv.cat](mailto:carme.guell@urv.cat) (C. Güell).

carboxymethyl cellulose) compared to the use of traditional dairy proteins (whey protein and sodium caseinate). This biopolymer is a negatively charged electrostatic protein-polysaccharide complex that is reported to form a thicker oil-water interface (Berendsen et al., 2014) and shown to enhance lemon oil chemical stability in emulsions produced with Shiratsu porous glass (SPG) membranes (Kaade et al., 2022). Since scale-up is challenging with SPG membranes, this study focusses on the performance of the DMTS emulsification process in terms of productivity (fluxes), droplet size distribution, and stability of the emulsions. Moreover, the study ascertains how the structure of the membrane can be tuned to reduce the energy input while maintaining the flux and the emulsion characteristics. Finally, to establish the most appropriate process conditions, a scaling relation predicting the effect of the DMTS system characteristics on droplet break-up is developed.

## 2. Materials and methods

To produce the simple oil-in-water emulsions, distilled water was used, and the lemon oil was purchased from Dallant, Spain. The emulsifiers used were whey protein isolate, WP (97.6%, Davisco Foods International, USA), sodium caseinate, NaCaS, (CAS: 9005-46-3, Sigma-Aldrich Quimica SL, Spain), and a protein-polysaccharide electrostatic complex: whey protein-carboxymethyl cellulose (CMC). The CMC was purchased from Sigma-Aldrich Quimica SL, Spain (CAS: 900-32-4). As for the DMTS, the nickel micro-sieves were provided by Stork Veco (Eerbeek, The Netherlands) and the micro-beads were purchased from Unicorn Industrial Cleaning Solutions (The Netherlands) (micro-beads size: 99  $\mu\text{m}$ ) and Microspheres-Nanospheres (USA) (micro-beads sizes: 42 and 68  $\mu\text{m}$ ). Sodium hydroxide and 1 M hydrochloric acid (HCl) were purchased from Fisher Scientific (UK) and acetic acid 96% was purchased from PanReac (Spain).

### 2.1. Continuous phase preparation

The continuous phases containing the proteins were prepared one day before using them for emulsification and stored overnight in the refrigerator (4 °C). The three emulsifiers used in this study were 1% wt WP, 1% wt NaCaS and 0.5% wt WP - 0.25% wt CMC electrostatic complex. Solutions (200 mL) of 2% wt WP and NaCaS were prepared and diluted on the day of the experiment to 1% wt. The pH of 1% wt WP and NaCaS were 6.8 and 6.5, respectively. As for the WP-CMC complex, 2% wt WP and CMC solutions were prepared the day before, and on the day of the experiment 200 mL of the complex was prepared by mixing the following: 22.5 g of 2% wt CMC, 22.5 g of distilled water, 90 g of 20 mM acetic acid buffer, and finally 45 g of 2% wt WP. At this point, the pH of the complex was adjusted to 3.8 with 1 M HCl. Berendsen et al. (2014) have shown that this protein-polysaccharide 2:1 ratio is soluble at pH 3.8 and that the complex is negatively charged (Berendsen et al., 2014).

### 2.2. Emulsification

To produce the 20% lemon oil-in-water emulsions, the same procedure reported by (Kaade et al. (2020)) was followed. In short, the continuous phase (80% wt), containing one of the three emulsifiers, and lemon oil (20% wt) were mixed to form 120–200 g emulsions. These emulsions were first homogenized by a high shear mixer (IKA® T-18 basic Ultra-turrax) at 15,500 rpm for 3 min to produce a coarse emulsion (a.k.a. premix). The average oil droplet size ( $d_{3,2}$ ) and span of the three coarse emulsions prepared, measured as explained in section S2 (supplementary materials), varied depending on the emulsifier used, and the values are given in Table 1.

This premix was then passed, five consecutive times (cycles), under constant pressure of 450 kPa, through a DMTS system to refine the emulsion that was then collected in an Erlenmeyer flask placed on a balance connected to a computer (Fig. 1). Consequently, mass versus

**Table 1**

Coarse emulsions' characterization. Different letters mean significant differences ( $p < 0.05$ ). Mean values are presented with the standard deviations.

Emulsifier	$d_{3,2}$ ( $\mu\text{m}$ )	Span (-)
WP	13.08 <sup>a</sup> $\pm$ 0.76	0.96 <sup>a</sup> $\pm$ 0.03
NaCaS	17.19 <sup>b</sup> $\pm$ 0.45	0.93 <sup>a</sup> $\pm$ 0.03
WP-CMC	19.95 <sup>c</sup> $\pm$ 0.96	0.93 <sup>a</sup> $\pm$ 0.02

time information was collected. This information is used to calculate mass flow rate,  $\varphi$ . Then, transmembrane flux,  $J$ , can be calculated using Equation (1).

$$J = \frac{\varphi}{\rho_e A_{column}} \quad (1)$$

Where  $A_{column}$  is the surface area of the microporous layer (177  $\text{mm}^2$ ),  $\rho_e$  is the emulsion density (972  $\text{kg}/\text{m}^3$ ) calculated using Equation (2). The continuous ( $\rho_c = 1003 \text{ kg}/\text{m}^3$ ) and oil phase ( $\rho_d = 846.2 \text{ kg}/\text{m}^3$ ) densities were measured using hydrometers.

$$\rho_e = \theta_d \rho_d + (1 - \theta_d) \rho_c \quad (2)$$

Where  $\theta_d$  is the dispersed phase volume fraction.

After each emulsification cycle, a sample was collected for droplet size distribution measurements.

The DMTS system used in this study is the same one previously used by Kaade et al. (2020) (Fig. 1), with a layer of silica glass micro-beads placed on top a nickel micro-sieve. In this study, three micro-beads sizes were tested to build the microporous layer: 99, 68 and 42  $\mu\text{m}$ , which will result in different interstitial void diameter (equation (6)). Also, by controlling the mass of the micro-beads placed on top of the nickel micro-sieve, it is possible to control the height of the microporous layer. In that sense, by adding 0.5, 1, 2 and 4 g of micro-beads, bed heights of 2.18, 4.35, 8.7 and 17.4 mm were obtained and tested for emulsification. The bed height can be calculated using Equation (3) (Van Der Zwan et al., 2008).

$$H = \frac{\text{mass of beads}}{\rho_p A_{column} (1 - \varepsilon)} \quad (3)$$

The porosity of the bed,  $\varepsilon$ , is calculated as:

$$\varepsilon = 1 - \frac{\rho_b}{\rho_p} \quad (4)$$

Here  $\rho_b$  and  $\rho_p$  are the micro-beads bulk and particle density, respectively. All the values of these parameters are reported in Table 2. The tortuosity of a bed of spherical particles is calculated using Equation (5).

$$\tau = 1 + 0.41 \ln\left(\frac{1}{\varepsilon}\right) \quad (5)$$

The pores in the microstructured system are assumed to have a diameter equivalent to the interstitial void diameter of the bed,  $d_v$ , defined by Equation (6) (Nazir et al., 2013).  $A_v$  is a ratio of a particle's surface area to its volume, and it is given by:  $A_v = 6/d_b$  where  $d_b$  is the micro-bead diameter.

$$d_v = \frac{4 \varepsilon}{A_v (1 - \varepsilon)} \quad (6)$$

Henceforth, the controlling parameters of the DMTS system will be referred to as interstitial void diameter and bed height.

A summary of all the experimental conditions used for refining coarse emulsions is reported in Table 3. In the first column of this table, experimental conditions reported by Kaade et al. (2020) were also added for future references and comparisons.

An extra set of emulsions was also produced using a tuned DMTS system to mimic an asymmetric membrane. In the tuned DMTS system

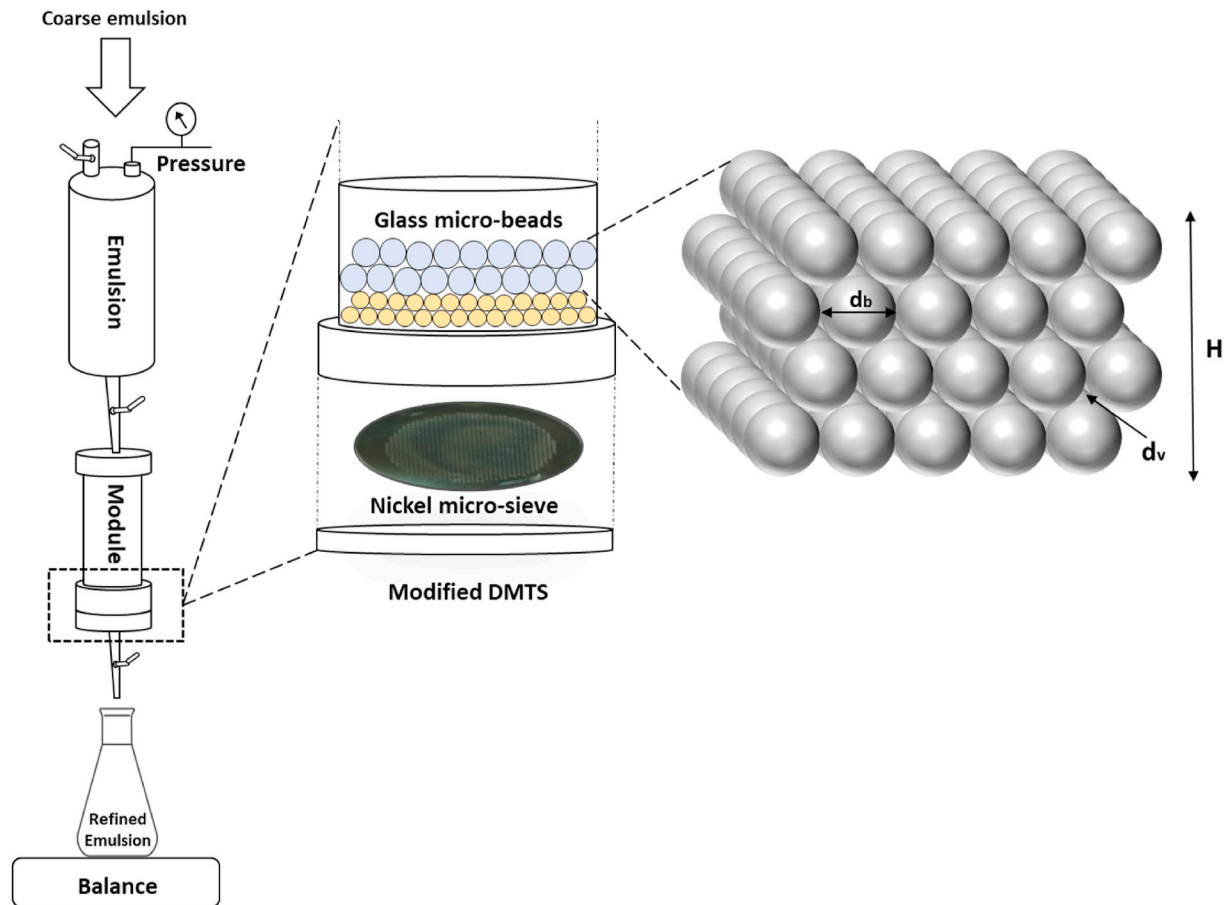


Fig. 1. Dynamic membrane setup with a microscopic representation of micro-beads size ( $d_b$ ), the interstitial void diameter ( $d_v$ ) and the bed height ( $H$ ).

**Table 2**  
Physical properties of the DMTS system.

	Micro-beads size, $d_{3,2}$ ( $\mu\text{m}$ )	Span of beads	Micro-beads density, $\rho_d$ , ( $\text{kg}\cdot\text{m}^{-3}$ )	Bulk density, $\rho_b$ , ( $\text{kg}\cdot\text{m}^{-3}$ )	Porosity of bed, $\epsilon$ , (%)	Interstitial void diameter, $d_v$ , ( $\mu\text{m}$ )	Tortuosity ( $\tau$ )	Bed height (mm)/ Amount (g)
DMTS 1	41.7	0.82	2466	1221	50.48	28.33	1.28	9.27/2
DMTS 2	67.5	0.65	2743	1474	46.28	38.79	1.32	7.68/2
DMTS 3	98.7	0.75	2446	1301	46.83	57.97	1.31	2.18/0.5
DMTS 4								4.35/1
DMTS 7								8.70/2
DMTS 8								17.4/4
Layering	Top layer: 98.7	0.75	2446	1301	46.83	57.97	1.31	4.35/1
	Bottom layer: 41.7	0.82	2466	1221	50.48	28.33	1.28	4.63/1

instead of having only one layer of micro-beads on top of the micro-sieve, two superimposed layers of micro-beads of different sizes were used. Specifically, the tuned DMTS comprised of, from bottom to top, the nickel micro-sieve followed by 1 g of 42  $\mu\text{m}$  sized micro-beads followed by 1 g of 99  $\mu\text{m}$  sized micro-beads. The exact method of preparation is reported in Kaade et al. (2020) (Fig. 1).

### 3. Results and discussion

#### 3.1. Effect of the DMTS system characteristics on the droplet size distribution of lemon oil emulsions stabilized with biopolymers

Lemon oil emulsions stabilized with Tween20 have been successfully produced using the DMTS system (Kaade et al., 2020). To produce emulsions stabilized with natural biopolymers such as WP and NaCaS, and a tailor-made biopolymer such as WP-CMC, the pressure was maintained at 450 kPa, and bed height and interstitial void diameter

were changed according to the information provided in Table 3. Fig. 2 shows  $d_{3,2}$  and span evolution during emulsification using these three emulsifiers (i) at four different bed heights (2.18, 4.35, 8.70 and 17.40 mm) using a constant interstitial void diameter of 57.97  $\mu\text{m}$ , and (ii) for three different interstitial void diameters maintaining the bed height at  $8.55 \pm 0.8$  mm. Similar to what was previously seen for emulsions with Tween20, there is a reduction of  $d_{3,2}$  during emulsification regardless of the emulsifier, bed height, and interstitial void diameter, with the highest size reduction occurring in the first emulsification cycle. Moreover, the droplet size of the coarse emulsion varies depending on the emulsifier. Emulsions stabilized with WP showed the smallest size (13.08  $\mu\text{m}$ ) and the ones stabilized with the WP-CMC complex resulted in the largest droplets (19.95  $\mu\text{m}$ ). It is acknowledged that small emulsifiers travel faster to the newly formed interfaces and can pack more tightly (Berendsen et al., 2014). Looking at the size of the three biopolymers used in this study, the following trend is reported: WP < NaCaS < WP-CMC (Bonilla-Reyna et al., 2011; Ladjal Ettoumi et al.,

**Table 3**

Experimental conditions (micro-beads mass, micro-beads size, droplet size of the coarse emulsion) used to refine 20% lemon oil emulsions at 450 kPa, and the porosities of the micro-sieves holding each silica beads.

	Tween20 <sup>a</sup>	WP	NaCaS	WP-CMC
Micro-sieve Porosity	2 g-42 μm – 5.7 μm 2.39%	2 g-42 μm – 13 μm 2.39%	2 g-42 μm – 17 μm 2.39%	Not possible
Micro-sieve Porosity	2 g-68 μm – 5.7 μm 2.39%	2 g-68 μm – 13 μm 2.39%	2 g-68 μm – 17 μm 2.39%	2 g-68 μm – 20 μm 2.33%
Micro-sieve Porosity	2 g-99 μm – 5.7 μm 1.31%	2 g-99 μm – 13 μm 1.31%	2 g-99 μm – 17 μm 1.31%	2 g-99 μm – 20 μm 2.33%
Micro-sieve Porosity	0.5 g-99 μm – 5.7 μm 2.39%	0.5 g-99 μm – 13 μm 2.33%	0.5 g-99 μm – 17 μm 2.39%	0.5 g-99 μm – 20 μm 2.33%
Micro-sieve Porosity	1 g-99 μm – 5.7 μm 1.31%	1 g-99 μm – 13 μm 1.31%	1 g-99 μm – 17 μm 1.23%	1 g-99 μm – 20 μm 2.33%
Micro-sieve Porosity	4 g-99 μm – 5.7 μm 1.31%	4 g-99 μm – 13 μm 1.31%	4 g-99 μm – 17 μm 1.23%	4 g-99 μm – 20 μm 2.33%
Micro-sieve Porosity	2 g-99 μm – 5.7 μm 2.33%			
Micro-sieve Porosity	2 g-99 μm – 5.7 μm 2.82%			
Micro-sieve Porosity	2 g-99 μm – 24 μm 2.33%			

<sup>a</sup> The experimental conditions in the first column are obtained from (Kaade et al., 2020).

2017), which agrees with the droplet size distribution of the coarse emulsions. Besides, from the dynamic interfacial tension profile (measurement description in section S1) (Fig. 3), and especially in the first few seconds, WP seems to lower the interfacial tension quicker than the other two biopolymers (NaCaS and WP-CMC) allowing the formation of smaller oil droplets. It is assumed that WP-CMC took a longer time to reach equilibrium because of the larger size of the complex molecule migrating to the oil-water interface. The span values of the coarse emulsions were similar regardless of the biopolymer used to stabilize the emulsion (Table 1).

It is noteworthy to mention that interfacial tension between lemon oil and water is lower than expected but that is due to the presence of emulsifying compounds in lemon oil like acetyl groups and methyl esters (Verkempinck et al., 2018). Also, (Rao and McClements 2012b) reported a lemon oil-water equilibrium interfacial tension of 8.3 mN m<sup>-1</sup> due to the high presence of surface-active compounds.

For the effect of the bed height, the highest size reduction always corresponds to the thinnest bed, and it is about 60% for the first cycle, regardless of the emulsifier. The increase in the thickness of the bed results in a lower size reduction, about 28–33%, again for the first cycle regardless of the emulsifier. Fig. 2 shows the span values and here it should be noted that all the emulsions produced were monomodal by the 5th emulsification cycle. However, WP and NaCaS stabilized emulsions show an increase in the span from the coarse emulsion to the one after the first emulsification cycle, followed by a slight decrease in the following emulsification cycles. Yet, for the emulsions stabilized with WP-CMC electrostatic complex, the span increases after each emulsification cycle, regardless of the thickness of the bed. So far, the results prove that the DMTS system is a powerful tool for producing emulsions with span values between 0.8 and 1.3, which is an important factor in terms of emulsion stability.

The size of the microbeads and the porosity of the bed determine the interstitial void diameter (Equation (6)), which is related to the size of the open interconnected channels in the system where droplet refinement occurs. The microbeads sizes used were 99, 68 and 42 μm, which correspond to  $d_v$  values of 57.97, 38.79 and 28.33 μm, respectively. It is important to note that the size of the coarse emulsions was always smaller than the interstitial void diameter, and even in this scenario, significant droplet break-up occurs (Fig. 2), which is indicative of the efficacy of this particular emulsification system. However, when the emulsions were stabilized with the WP-CMC complex, emulsion refinement was not possible with the microporous system using 42 μm microbeads ( $d_v = 28.33$  μm). In this case, the pressure applied was not enough to overcome the resistance of the bed and the higher viscosity of

the continuous phase attributed to the presence of the CMC. Moreover, it has been shown that when refining lemon oil emulsions using only the nickel micro-sieve, for the emulsion to pass through the micro-sieve, the ratio of the coarse emulsion diameter to the diameter of the open pore in the micro-sieve should be lower than 1. If this condition is not fulfilled, the micro-sieve will foul significantly after the first cycle, completely blocking the pores. In the present study, the highest  $d_{coarse}/d_v$  assessed is that of the WP-CMC stabilized emulsions refined through the bed of 42 μm microbeads ( $d_{coarse}/d_v = 0.7$ ). Even though the literature reports a successful production of W/O/W double emulsions with a higher  $d_{coarse}/d_v$  ratio ( $\approx 0.92$ ) (Wang et al., 2020), those emulsions did not contain a viscosity modifying agent like the CMC in our case.

To better understand the effects of the interstitial void diameter and bed height on droplet break-up and to account for the different size of the coarse emulsions for each biopolymer,  $d_{3,2}/d_{coarse}$  and span values from the 5th emulsification cycle were plotted versus bed height and  $d_v$  (Fig. 4). It is clear from Fig. 4a and c that the thicker the bed and the smaller the interstitial void diameter, the less droplet break-up happens. It should be highlighted that with the thinnest bed, an 80% size reduction of the coarse emulsions was achieved, for the three emulsifiers (Fig. 4a).

When the DMTS system is composed of a thick bed and/or small micro-beads, transmembrane flux drops because of the higher resistance which also decreases the shear inside the bed pores responsible for deforming and breaking oil droplets (Nazir et al., 2013; Sawalha et al., 2016). Regarding span values, Fig. 4b shows that thicker beds gave higher span values probably because they allow droplets to reside in the bed for longer periods allowing them to re-coalesce (Laouini et al., 2014). However, results in Fig. 4d indicate that large interstitial void diameters, which give the smallest droplets (Fig. 4c), are less efficient in producing emulsions with a narrow droplet size distribution, that is, having higher span values.

Comparison of the droplet size distribution of the emulsions obtained in this study to the literature remains limited for lack of similarities. Berendsen et al. (2014) produced sunflower O/W emulsions with a premix membrane emulsification technique (SPG membrane) stabilized with 1 %wt WP and 0.5%wt WP - 0.25%wt CMC. The membrane pore diameter was 10 μm and the  $d_{coarse}/d_v$  ratio was 7. Although they report a higher droplet size reduction (94%) after four emulsification cycles (reported  $d_{4,3}$  about 10 μm), they obtained span values of 1.7 and 3.6 for WP and WP-CMC, respectively (Berendsen et al., 2014), which are higher than the ones obtained in the present case for lemon oil and the DMTS system (1 and 1.1 for 1 %wt WP and 0.5 %wt WP - 0.25 %wt CMC, respectively). This is yet another major asset for DMTS and its ability to

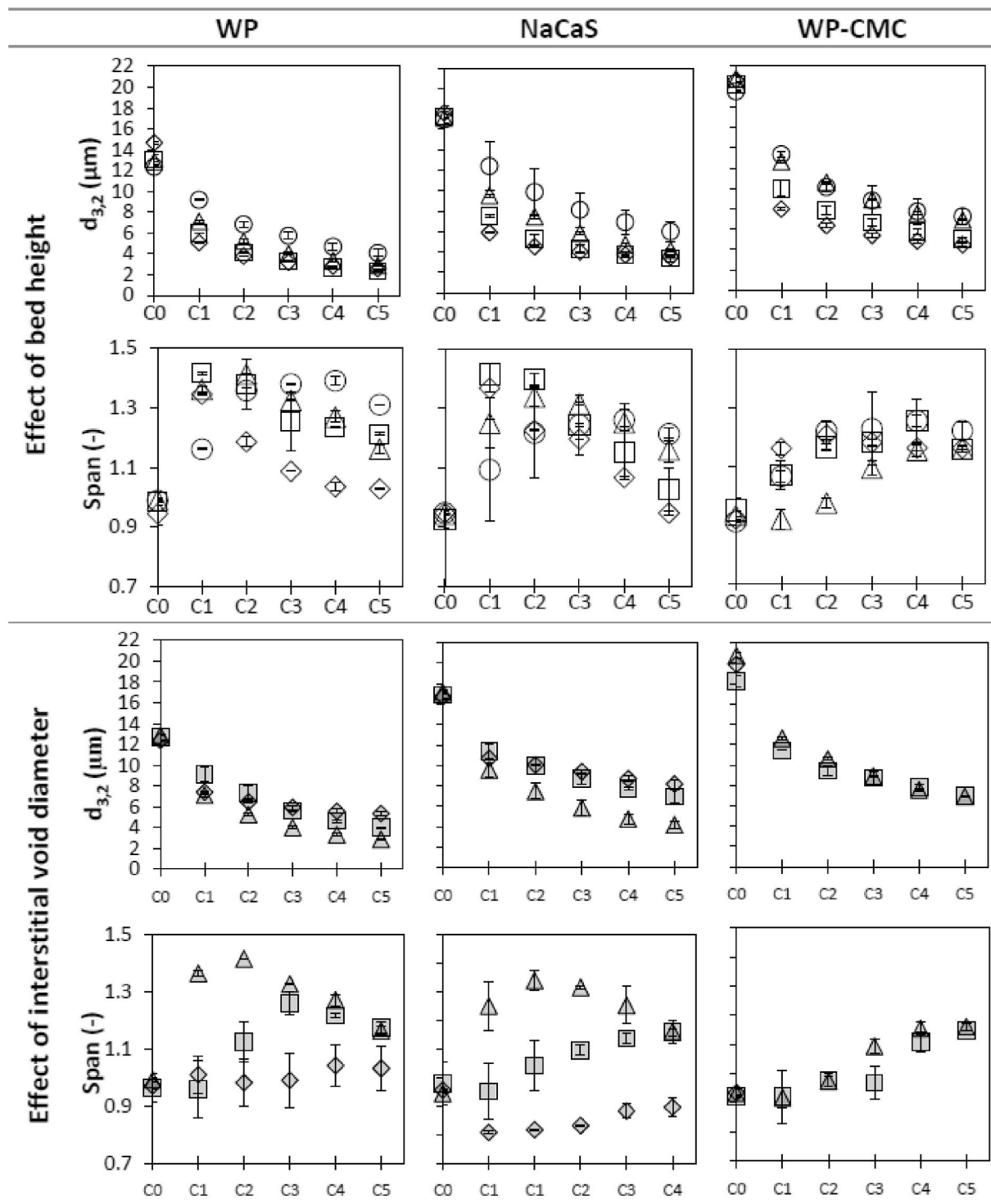


Fig. 2. Effect of emulsifier type, micro-beads size (maintaining bed height at 8.55 mm), bed height (maintaining interstitial void diameter at 57.97  $\mu\text{m}$ ) and emulsification cycles on Sauter mean diameter and span. Markers:  $\circ$ : 2.18 mm,  $\triangle$ : 4.35 mm,  $\square$ : 8.70 mm,  $\diamond$ : 17.4 mm,  $\diamond$ : 28.33  $\mu\text{m}$ ,  $\square$ : 38.79  $\mu\text{m}$ ,  $\triangle$ : 57.97  $\mu\text{m}$ .

produce narrow droplet size emulsions even when using biopolymers to stabilize the emulsion. As for DMTS systems, the literature shows applications in premix mode to produce O/W and W/O/W emulsions stabilized with WP. Ladjal (Ladjal Ettoumi et al., 2017) report producing 20% sunflower oil-in-water emulsions stabilized with WP using a 2 mm bed of 71  $\mu\text{m}$  hydrophilic glass beads. They were able to refine a coarse emulsion ( $d_{4,3} = 23 \mu\text{m}$ ) at 300 kPa with five emulsification cycles to a

final size,  $d_{4,3}$ , of 5  $\mu\text{m}$ . As in our study, droplet break-up occurred mainly in the first cycle. Eisinaitė et al. (2016) encapsulated beetroot juice in  $W_1/O/W_2$  emulsions using 0.5% WP to stabilize the sunflower oil/ $W_2$  interphase (Eisinaitė et al., 2016). As for the conditions of the DMTS system, they were exactly the same than the ones used by (Ladjal Ettoumi et al. 2017) Starting from a coarse emulsion,  $d_{3,2}$ , of 32  $\mu\text{m}$  and span of 1.4, they were able to refine it down to 20  $\mu\text{m}$  and span of 5. The

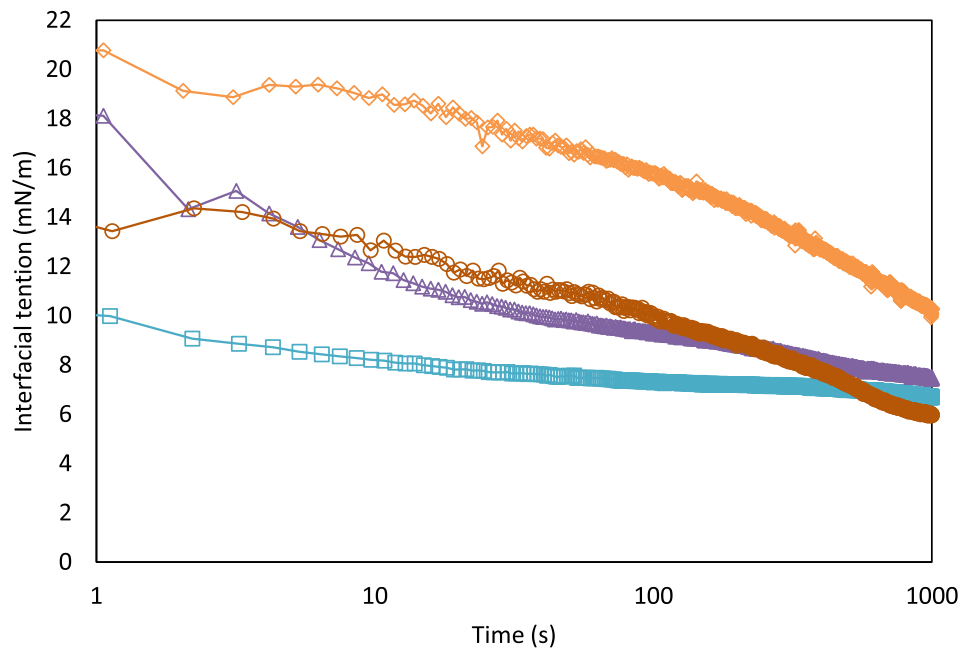


Fig. 3. Dynamic interfacial tension profile of lemon oil with (◇) water (□), WP (△), NaCaS and (○) WP-CMC solutions.

high span value at the end of the emulsification process might be due to the higher viscosity of sunflower oil (0.049 Pa s) compared to lemon oil (0.000923 Pa s), and also it has to be noted that stable double emulsions are more difficult to achieve than single O/W emulsions. Also, Wang et al. (2021a), using a 2 mm bed of 38  $\mu\text{m}$  glass-beads, produced  $W_1/O/W_2$  double emulsions (20% oil phase) (at 500 kPa) using 1 %wt WP to stabilize the sunflower oil/ $W_2$  emulsion. Starting with a  $d_{4,3}$  and span of 130  $\mu\text{m}$  and 2.1, respectively, for the coarse emulsion, the authors attained a  $d_{4,3}$  and span of 7.5  $\mu\text{m}$  and 0.8, respectively, for the refined emulsion after 3 emulsification cycles. The authors achieved a higher droplet size reduction of 94% primarily due to the large starting size of the coarse emulsion and the larger transmembrane pressure. These authors show, as in the present case, that the DMST system allows large droplet breakup with complex emulsion formulations with no significant fouling. Finally the only paper that uses the DMST system to stabilize lemon oil-in-water emulsions using WP is reported by Kaade et al. (2020); Kaade et al., 2022. The authors utilize an 8.3  $\mu\text{m}$  bed of 94.3  $\mu\text{m}$  glass-beads at a transmembrane pressure of 450 kPa to refine a 20% lemon oil-in-water coarse emulsion ( $d_{3,2}/\text{span} = 16 \mu\text{m}/0.9$ ) stabilized by 1 %wt WP. After 5 emulsification cycles the  $d_{3,2}$  and span were 3.5  $\mu\text{m}$  and 1.1, respectively. Both the droplet size reduction and the span are comparable to the ones obtained in our study.

To compare the extent of droplet break-up obtained in this study with previous literature, it is worth using the droplets' diameter ( $d_{3,2}$ ) to the interstitial void diameter ( $d_v$ ) ratio. It is clear that for all the emulsions in this study, the droplet size of all the coarse emulsions are smaller than the interstitial void diameter ( $d_{3,2}/d_v < 1$ ). Also, by the last emulsification cycle this ratio is  $0.05 < d_{3,2}/d_v < 0.2$  which is in the lowest range reported for premix membrane emulsification (Laouini et al., 2014; Nazir et al., 2013; Sawalha et al., 2016; Vladisavljević et al., 2004; Vladisavljević et al., 2006a). This again, shows the potential of the DMST emulsification technique.

### 3.2. Scaling equation for droplet size versus applied pressure in the DMST system

Several authors have related droplet break-up to the applied energy

through the energy density relation in emulsification systems to predict the droplet size based on the pressure applied (Nazir et al., 2013; Van Der Zwan et al., 2008). A scaling relationship, at a constant pressure of 450 kPa, is proposed to relate the structure of the microporous system (interstitial void diameter and bed height), the number of emulsification cycles ( $N$ ), and the nature of the emulsifier ( $d_{coarse}$ ) to the droplet size ( $d_{3,2}$ ) (Equation (7)).

$$\frac{d_{3,2}}{d_{coarse}} = a \cdot N^{-b} \cdot \left(\frac{H}{d_v}\right)^c \quad (7)$$

where  $a$ ,  $b$  and  $c$  are fitting parameters. The values of the three constants in Equation (7) were computed by the Solver tool in Microsoft Excel and verified with the Curve Fitting tool in Matlab (R2015a). To do so, the results from all the experimental conditions (Table 3) with the four emulsifiers (Tween 20, WP, NaCaS and WP-CMC), including all the replicates (255 points), were considered.

The fitting parameters are reported in Table 4, their p-values were:  $p \ll 0.001$ , which shows their statistical significance. Also, the general p-value of the equation was also:  $p \ll 0.001$ . The fit is very good ( $R^2 \approx 0.83$ ) considering the extent of experimental variables. Fig. 5 shows the experimental Sauter mean diameter plotted against the values obtained from Equation (7).

The importance of this equation is that it offers the possibility of either predicting the droplet size resulting when using a particular DMST configuration or designing the appropriate DMST system to obtain a specific droplet size for O/W emulsions stabilized by several biopolymers at a constant pressure of 450 kPa.

### 3.3. Tailored design of the DMST system

As previously reported by Kaade et al. (2020), it is possible to tailor-design the DMST system to maintain high emulsion through-put while decreasing the energy inputted, by reducing the emulsification cycles, and still obtain narrow droplet size distributions during the production of lemon oil emulsions stabilized with Tween 20. This modified system, referred to from here on as layered DMST, consists of two superimposed layers of microbeads of different size. As a result, the

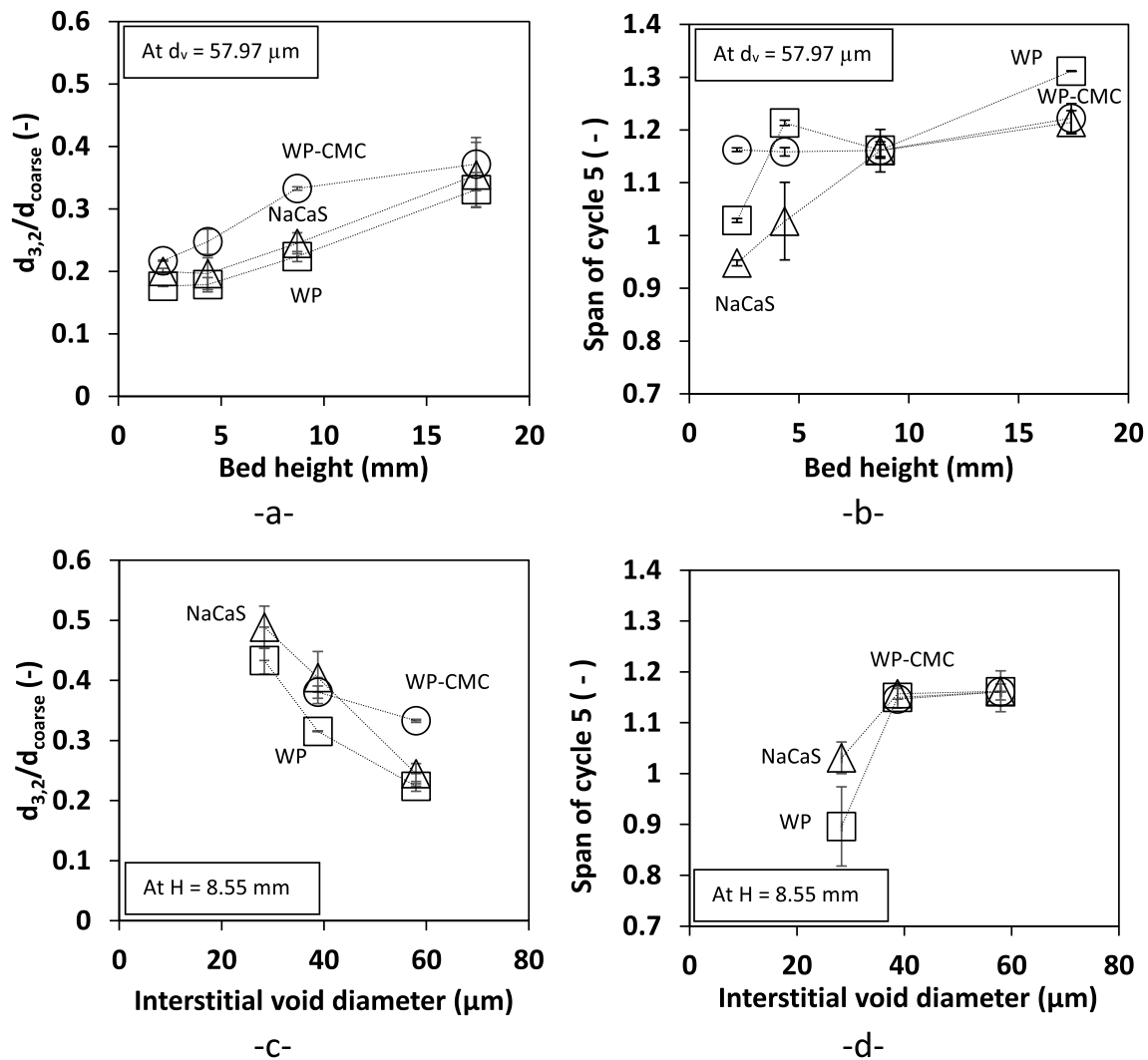


Fig. 4. Effects of bed height (a,b), interstitial void diameter (c,d) and emulsifier type on the droplet break-up and span of the last emulsification cycle of 20% LO emulsions. Markers: ○: WP-CMC; □: WP; △: NaCaS.

Table 4  
Regression parameters for Equation 7.

	Coefficient	STD
a	0.1387	$\pm 0.0100$
b	0.372	$\pm 0.0139$
c	0.2902	$\pm 0.0137$
R <sup>2</sup>	0.8249	

microstructured system has an upper layer (4.35 mm) of 57.97  $\mu\text{m}$  of interstitial void diameter and a bottom layer of the similar thickness (4.63 mm) with an interstitial void diameter of about 28.33  $\mu\text{m}$  (Table 2), resembling an asymmetric membrane, but with the more open porous structure in contact with the inlet emulsion.

A set of experiments was designed to test the performance of the layered DMTS system with emulsions stabilized with WP, NaCaS or WP-CMC complex. Lemon oil emulsions (20% wt) were prepared as described in section 2.2 and then they were refined at 450 kPa with the layered DMTS system. Fig. 6 shows the droplet break-up ( $d_{3,2}$ ,  $d_{3,2}/d_{\text{coarse}}$  and span) as well as the transmembrane flux of the lemon emulsions stabilized with the three biopolymers. Since one of the goals is to reduce the global energy input, the emulsion refinement with the layered DMTS was performed decreasing the emulsification cycles from 5 to 3; therefore, the results can be compared with the ones obtained

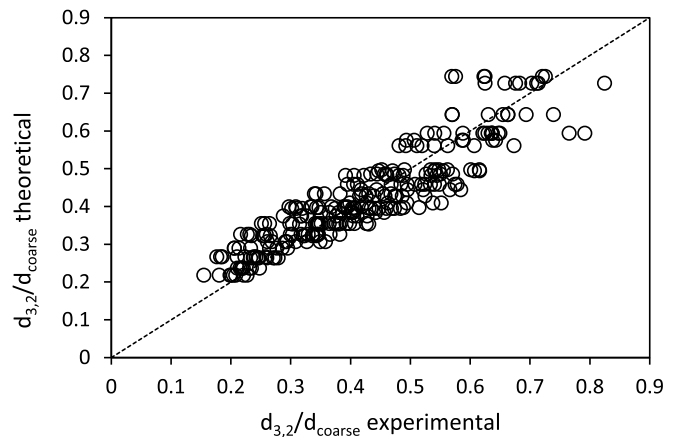


Fig. 5. Experimental  $d_{3,2}$  values plotted against the values obtained from Equation 7.

after three cycles using the standard DMTS system of similar thickness and intermediate interstitial void diameter (Fig. 2).

Looking at Sauter mean diameter ( $d_{3,2}$ ), different trends are observed depending on the emulsifier: WP gave higher  $d_{3,2}$  value than the one

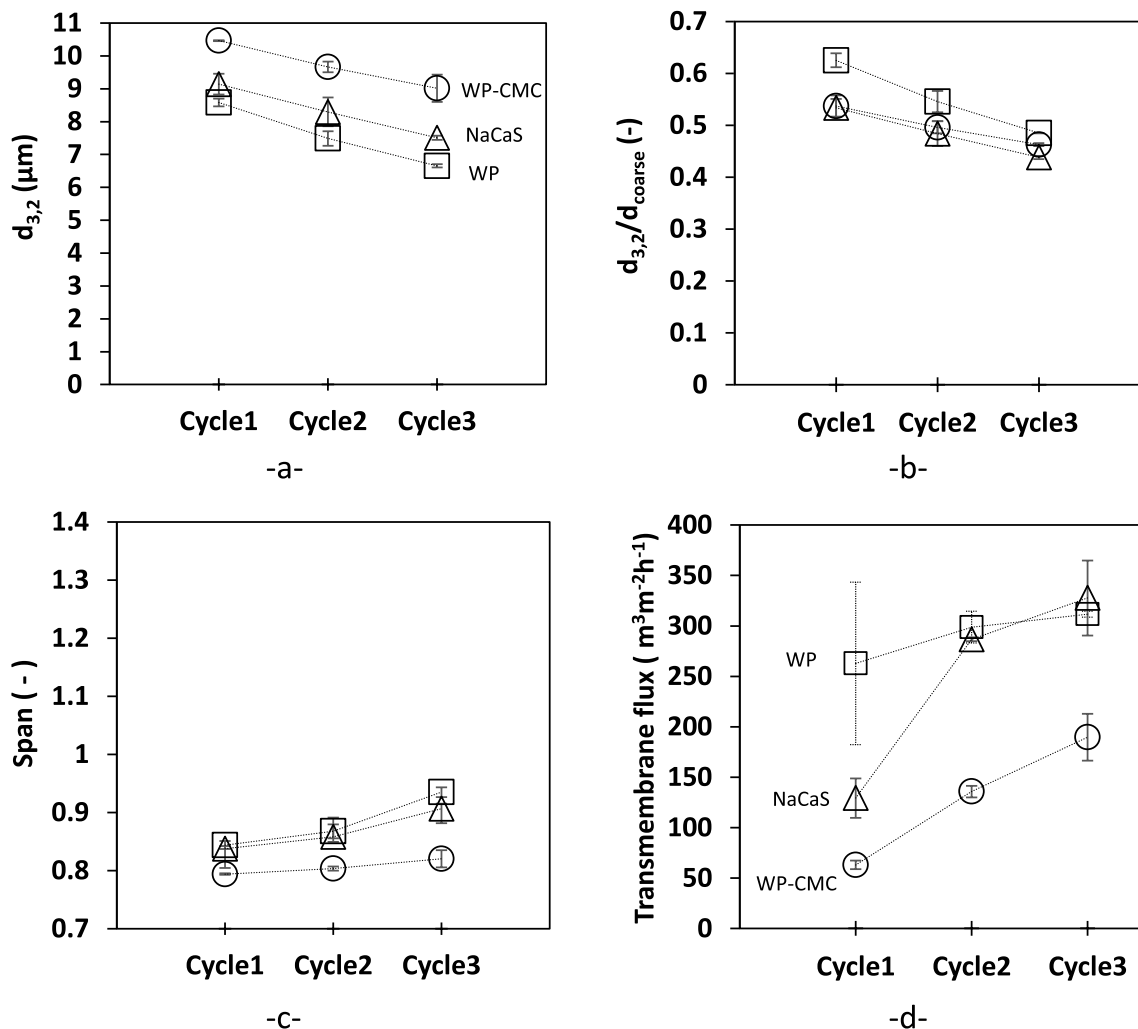


Fig. 6. Impact of using a layered DMTS system and a different emulsifier on (a,b) droplet break-up, (c) span and (d) transmembrane flux during the production of 20% LO emulsions. Markers:  $\circ$ : WP-CMC;  $\square$ : WP;  $\triangle$ : NaCaS.

obtained using a 9.27 mm bed of  $d_v = 68 \mu\text{m}$ , while for NaCaS and WP-CMC the  $d_{3,2}$  values were slightly lower or similar, respectively, to the ones with the mono-sized bed after 3 emulsification cycles. It is interesting to point out that, with the WP-CMC complex and as mentioned in section 3.1, the emulsion was not able to pass through the DMTS system composed with  $d_v = 28.33 \mu\text{m}$  microbeads, but with the layering arrangement this problem is overcome and the emulsions were able to be refined to a  $d_{3,2}$  value of about  $9 \mu\text{m}$ . It may be that the first layer with  $d_v = 57.79 \mu\text{m}$ , refines the WP-CMC lemon oil emulsion down to a droplet size that allows the emulsion to move through the tighter channels of the bottom layer, where they are further refined. Looking at Fig. 6b, and by the third cycle, the droplet size reduction was the same regardless of the emulsifier type.

As for the span values, all of them were lower than the ones resulting after three emulsification cycles with the 7.68 mm mono-sized bed of  $d_v = 38.79 \mu\text{m}$ , showing the potential of tailoring the microstructured system to obtain narrower droplet size distributions. To the authors' knowledge no other study has reported producing emulsions stabilized with WP-CMC with a span value as small as 0.82. For reference, sunflower oil (Berendsen et al., 2014) and lemon oil (Kaade et al., 2022) emulsions stabilized with the same WP-CMC complex and emulsified with an SPG membrane resulted in span values of 3.5 and 1.4 respectively. As for the resulting transmembrane fluxes, the results are commented in the next section and compared with the ones obtained with the monosized DMTS system.

### 3.4. Effect of the DMTS and layered DMTS systems characteristics on the emulsification flux

As mentioned previously, 20% lemon oil emulsions were refined through the DMTS system with a constant pressure of 450 kPa, while varying interstitial void diameters (28.33, 38.79, and 57.97  $\mu\text{m}$ ), bead height (2.18, 4.35, 8.70 and 17.40 mm) and emulsifier type (WP, NaCaS, and WP-CMC). Data collected during emulsification allows the calculation of the transmembrane flux (Equation (1)). Fig. 7 shows the fluxes as a function of the emulsification cycles for the different conditions.

Regarding the influence of the bed thickness, it is clear from Fig. 7a-c that the highest flux value is obtained for the thinnest DMTS system. The flux value obtained, at the fifth cycle, was around  $1000 \text{m}^3 \text{m}^{-2} \text{h}^{-1}$  for emulsions stabilized with WP or WP-CMC, while it was close to  $900 \text{m}^3 \text{m}^{-2} \text{h}^{-1}$  for emulsions stabilized with NaCaS. These values are in the upper range of the ones reported for DMTS emulsification and very similar to the ones obtained with the exact same oil type and fraction, pressure, and microporous bed conditions but with Tween20 as emulsifier (Kaade et al., 2020). Therefore, the use of biopolymers (natural or tailor-made) does not seem to cause extensive fouling in the DMTS system reducing the productivity. A recent study reported the use of ceramic membranes (1 mm thick and pore sizes 1–2  $\mu\text{m}$ ) to produce simple O/W emulsions at 500 kPa, stabilized with Tween®80, in premix mode (Nishihora et al., 2020). This system could be considered similar to ours because the DMTS is an interconnected porous system similar to



**Fig. 7.** Effects of bed height (a,b,c) and interstitial void diameter (d,e,f) on transmembrane flux during emulsification of lemon oil (20%) stabilized with WP, NaCaS and WP-CMC complex. Markers: ○: 2.18 mm; □: 4.35 mm; ◇: 8.7 mm; △: 17.4 mm; □: 28.33 μm; ●: 38.79 μm; ◇: 57.97 μm.

that of a ceramic membrane. After two emulsification cycles, where the major break-up occurred after the first cycle, they obtained a 65% droplet size reduction and a span of 0.82. Although the emulsion had a smaller size distribution than the one obtained in this study so far, the droplet size reduction (65%) is still low compared to the results discussed in section 3.1 (80%). Moreover, the transmembrane flux obtained with the ceramic membrane ( $19 \text{ m}^3 \text{ m}^{-2} \text{ h}^{-1}$ ) that is half as thick as the thinnest bed tested in this study, is 52 times lower than that with the DMTS system ( $1000 \text{ m}^3 \text{ m}^{-2} \text{ h}^{-1}$ ). This demonstrates the potential of emulsification with DMTS for industrial applications, since it achieves the production of monodisperse emulsions with flux values of industrial significance.

The results in Fig. 7 show that the thicker the bed and the smaller the interstitial void diameters the lower the transmembrane fluxes, which can be explained by the higher resistance of these particular configurations (Sawalha et al., 2016). Nonetheless, some discrepancies are noticeable in the plots showing the flux values for WP and NaCaS stabilized emulsions. Fig. 7 a-b show a much higher flux value for the

system with the thinnest bed, while in Fig. 7 d-e it can be seen that fluxes obtained with the  $99 \mu\text{m}$  beads are in same range than the ones obtained with the  $68 \mu\text{m}$  beads. This behavior can be explained by the different porosity of the micro-sieves used to support the bed (Table 3). The DMTS system consist of a bed with a porosity of about 50%, supported by a nickel micro-sieve with a much lower porosity (1.2–2.4%), exhibiting higher resistance, but not contributing to droplet break up. As reported previously by Kaade et al. (2020), for the same microporous systems characteristics, higher porosities of the nickel sieve (acting as a support) result in higher fluxes and the opposite is true; however, while also maintaining the same microporous system characteristics, changing the nickel sieve porosity has no effect on droplet breakup. The effect of the porosity of the micro-sieve is overlooked in the DMTS emulsification literature, and controlling this factor has the potential of optimizing transmembrane flux, while maintaining all the other operational parameters. Comparing the effect of the emulsifiers on the transmembrane fluxes, it is clear that emulsions with WP and NaCaS behaved similarly in comparison to emulsions with the protein-polysaccharide complex. This

latter had flux values at the first emulsification cycle lower than the other two emulsifiers mainly because of the higher emulsion viscosity.

As emulsification progresses, increasing the number of cycles, the flux values increased, especially for WP-CMC stabilized emulsions. A possible explanation is that the emulsions undergo shear-thinning. (Nor Hayati et al., 2009) report that O/W emulsions containing CMC exhibit shear thinning behavior. As for the emulsions with WP and NaCaS, the observed trend is opposite, with a decrease of the flux regardless of the thickness of the microporous systems. Since the oil droplets in their emulsions are smaller than those with the complex, Sahin et al. (2014) explain that with the increasing number of cycles, and thus decreasing size and increasing number of droplets, oil droplets might slightly accumulate in or before the bed, thus fouling the bed and in turn lowering the flux values.

Emulsion refinement leading to narrow droplet size distributions while reducing the energy input need to be accompanied by high productivities to scale-up the process. Fig. 6d shows the flux evolution during emulsification in the layered DMTS system for the three emulsifiers. The flux values at the 3rd cycle are of around  $300 \text{ m}^3 \text{ m}^{-2} \cdot \text{h}^{-1}$  for emulsions stabilized with WP and NaCaS, and about  $200 \text{ m}^3 \text{ m}^{-2} \cdot \text{h}^{-1}$  for emulsions stabilized with WP-CMC. Even though these values are 40% lower than the ones obtained with the 9.27 mm bed of  $68 \mu\text{m}$  microbeads, they are still comparable to flux values reported for Shiratsu porous glass membranes (Vladisavljević et al., 2006b).

#### 4. Conclusions

This study has proven the feasibility of using standard and layered DMTS systems to produce lemon oil emulsions stabilized by two milk proteins (whey protein and sodium caseinate) and a protein-polysaccharide electrostatic complex (WP-CMC). It has been established that tailoring the operating parameters of the DMTS system (interstitial void diameter, bed height, nickel micro-sieve porosity) enabled to control the droplet size distribution while maintaining the emulsion productivity. Overall, for the three emulsifiers, the thinner the bed the smaller and narrower size distribution of the droplets. As for the interstitial void diameter, it was clear that increasing this parameter, droplet size decreased and increased the droplet size distribution. A scaling relation to predict the droplet size based on the size of the coarse emulsion, the number of emulsification cycles, and the ratio between bed height and interstitial void diameter was established to be used for process scale-up. The results show the potential of the DMTS system to refine emulsions stabilized with biopolymers, since at the fifth emulsification cycle the values of  $d_{3,2}/d_v$  are in the lowest range reported for premix emulsification, while maintaining the productivity at  $300\text{--}200 \text{ m}^3 \text{ m}^{-2} \text{ h}^{-1}$ . The layered DMTS system allows to tailor the microstructure to refine the emulsion while reducing the energy input. The layered DMTS allowed the production of a monodispersed emulsion, stabilized with WP-CMC complex, with the lowest reported span value (0.82) so far. The type of tuning of the microporous system applied in the present work is a promising technology to produce stable emulsions with a narrow droplet size distribution and high through-put while reducing the energy input.

#### Credit author statement

Wael Kaade: Conceptualization, Methodology, Investigation, Writing – original draft. Carme Güell: Conceptualization, writing, review, and editing, Supervision. Silvia De Lamo-Castellví: Conceptualization. Montse Ferrando: Conceptualization, Writing – review & editing, Supervision.

#### Declaration of competing interest

The authors declare that they have no known competing financial interests or personal relationships that could have appeared to influence

the work reported in this paper.

#### Data availability

Data will be made available on request.

#### Acknowledgments

The authors acknowledge financial support provided by Ministerio de Economía y Competitividad - CTQ 2014-54520-P, by Ministerio de Ciencia e Innovación, Spain - PGC 2018-097095-B-I00. Wael Kaade reports financial support was provided by Ministerio de Ciencia e Innovación, Spain - Subprograma Nacional de Formación BES-2015-072051. The authors thank Stork Veco (Eerbeek, the Netherlands) for providing the nickel microsieves.

#### Appendix A. Supplementary data

Supplementary data to this article can be found online at <https://doi.org/10.1016/j.jfoodeng.2023.111620>.

#### References

- Bai, L., Huan, S., Li, Z., McClements, D.J., 2017. Comparison of emulsifying properties of food-grade polysaccharides in oil-in-water emulsions: gum Arabic, beet pectin, and corn fiber gum. *Food Hydrocolloids* 66, 144–153. <https://doi.org/10.1016/j.foodhyd.2016.12.019>.
- Berendsen, R., Güell, C., Henry, O., Ferrando, M., 2014. Premix membrane emulsification to produce oil-in-water emulsions stabilized with various interfacial structures of whey protein and carboxymethyl cellulose. *Food Hydrocolloids* 38, 1–10. <https://doi.org/10.1016/j.foodhyd.2013.11.005>.
- Bonilla-Reyna, B., Sosa-Herrera, M.G., Martínez-Padilla, L.P., 2011. Interfacial adsorption and shear flow properties of gum Arabic-sodium caseinate mixtures. *Procedia Food Science* 1, 12–16. <https://doi.org/10.1016/j.profoo.2011.09.003>.
- Dragosavac, M.M., Holdich, R.G., Vladisavljević, G.T., Sovilj, M.N., 2012. Stirred cell membrane emulsification for multiple emulsions containing unrefined pumpkin seed oil with uniform droplet size. *J. Membr. Sci.* 392 (393), 122–129. <https://doi.org/10.1016/j.memsci.2011.12.009>.
- Eisinaite, V., Juraite, D., Schroën, K., Leskauskaitė, D., 2016. Preparation of stable food-grade double emulsions with a hybrid premix membrane emulsification system. *Food Chem.* 206, 59–66. <https://doi.org/10.1016/j.foodchem.2016.03.046>.
- Joscelyne, S.M., Trägårdh, G., 1999. Food emulsions using membrane emulsification: conditions for producing small droplets. *J. Food Eng.* 39 (1), 59–64. [https://doi.org/10.1016/S0260-8774\(98\)00146-0](https://doi.org/10.1016/S0260-8774(98)00146-0).
- Kaade, W., Güell, C., Ballon, A., Mellado-Carretero, J., De Lamo-Castellví, S., Ferrando, M., 2020. Dynamic membranes of tunable pore size for lemon oil encapsulation. *LWT (Lebensm.-Wiss. & Technol.)*, 109090. <https://doi.org/10.1016/j.lwt.2020.109090>.
- Kaade, W., Méndez-Sánchez, C., Güell, C., De Lamo-Castellví, S., Mestres, M., Ferrando, M., 2022. Complexed Biopolymer of Whey Protein and Carboxymethyl Cellulose to Enhance the Chemical Stability of Lemon Oil-In-Water Emulsions. *ACS Food Science & Technology*. <https://doi.org/10.1021/acscfoodscitech.1c00274>.
- Kandori, K., 1995. Chapter 7 - applications of microporous glass membranes: membrane emulsification. In: Gaonkar, A.G. (Ed.), *Food Processing*. Elsevier Science B.V, pp. 113–142. <https://doi.org/10.1016/B978-044481500-2/50009-8>.
- Ladjal Ettoumi, Y., Berton-Carabin, C., Chibane, M., Schroën, K., 2017. Legume protein isolates for stable acidic emulsions prepared by premix membrane emulsification. *Food Biophys.* 12 (1), 119–128. <https://doi.org/10.1007/s11483-017-9471-x>.
- Laouini, A., Charcosset, C., Fessi, H., Schroën, K., 2014. Use of dynamic membranes for the preparation of vitamin E-loaded lipid particles: an alternative to prevent fouling observed in classical cross-flow emulsification. *Chem. Eng. J.* 236, 498–505. <https://doi.org/10.1016/j.cej.2013.10.053>.
- Nazir, A., Boom, R.M., Schroën, K., 2013. Droplet break-up mechanism in premix emulsification using packed beds. *Chem. Eng. Sci.* 92, 190–197. <https://doi.org/10.1016/j.ces.2013.01.021>.
- Nazir, A., Maan, A.A., Sahin, S., Boom, R.M., Schroën, K., 2015. Foam preparation at high-throughput using a novel packed bed system. *Food Bioprod. Process.* 94 (August), 561–564. <https://doi.org/10.1016/j.fbp.2014.08.002>.
- Nazir, A., Vladisavljević, G.T., 2021. Droplet breakup mechanisms in premix membrane emulsification and related microfluidic channels. *Adv. Colloid Interface Sci.* 290 <https://doi.org/10.1016/j.cis.2021.102393>.
- Nishihora, R.K., Luhede, L., Fritsching, U., Novy Quadri, M.G., Hotza, D., Rezwan, K., Wilhelm, M., 2020. Premix membrane emulsification using flat microfiltration inorganic membranes with tailored structure and composition. *J. Membr. Sci.* 608 (January), 118124 <https://doi.org/10.1016/j.memsci.2020.118124>.
- Nor Hayati, I., Che Man, Y. Bin, Tan, C.P., Nor Aini, I., 2009. Droplet characterization and stability of soybean oil/palm kernel olein O/W emulsions with the presence of selected polysaccharides. *Food Hydrocolloids* 23 (2), 233–243. <https://doi.org/10.1016/j.foodhyd.2008.01.004>.

- Rao, J., McClements, D.J., 2012a. Impact of lemon oil composition on formation and stability of model food and beverage emulsions. *Food Chem.* 134 (2), 749–757. <https://doi.org/10.1016/j.foodchem.2012.02.174>.
- Rao, J., McClements, D.J., 2012b. Lemon oil solubilization in mixed surfactant solutions: rationalizing microemulsion & nanoemulsion formation. *Food Hydrocolloids* 26 (1), 268–276. <https://doi.org/10.1016/j.foodhyd.2011.06.002>.
- Sahin, S., Sawalha, H., Schroën, K., 2014. High throughput production of double emulsions using packed bed premix emulsification. *Food Res. Int.* 66, 78–85. <https://doi.org/10.1016/j.foodres.2014.08.025>.
- Sawalha, H., Sahin, S., Schroën, K., 2016. Preparation of polylactide microcapsules at a high throughput with a packed-bed premix emulsification system. *J. Appl. Polym. Sci.* 133 (24), 3–9. <https://doi.org/10.1002/app.43536>.
- Van Der Zwan, E.A., Schroën, C.G.P.H., Boom, R.M., 2008. Premix membrane emulsification by using a packed layer of glass beads. *AIChE J.* 54 (8), 2190–2197. <https://doi.org/10.1002/aic.11508>.
- Verkempinck, S.H.E., Kyomugasho, C., Salvia-Trujillo, L., Denis, S., Bourgeois, M., Van Loey, A.M., Hendrickx, M.E., Grauwet, T., 2018. Emulsion stabilizing properties of citrus pectin and its interactions with conventional emulsifiers in oil-in-water emulsions. *Food Hydrocolloids* 85 (July), 144–157. <https://doi.org/10.1016/j.foodhyd.2018.07.014>.
- Vladisavljević, G.T., Shimizu, M., Nakashima, T., 2004. Preparation of monodisperse multiple emulsions at high production rates by multi-stage premix membrane emulsification. *J. Membr. Sci.* 244 (1–2), 97–106. <https://doi.org/10.1016/j.memsci.2004.07.008>.
- Vladisavljević, G.T., Shimizu, M., Nakashima, T., 2006a. Production of multiple emulsions for drug delivery systems by repeated SPG membrane homogenization: influence of mean pore size, interfacial tension and continuous phase viscosity. *J. Membr. Sci.* 284 (1–2), 373–383. <https://doi.org/10.1016/j.memsci.2006.08.003>.
- Vladisavljević, G.T., Surh, J., McClements, J.D., 2006b. Effect of emulsifier type on droplet disruption in repeated Shirasu porous glass membrane homogenization. *Langmuir* 22 (10), 4526–4533. <https://doi.org/10.1021/la053410f>.
- Wang, J., Ballon, A., Schroën, K., de Lamo-Castellví, S., Ferrando, M., Güell, C., 2021a. Polyphenol loaded W1/O/W2 emulsions stabilized with lesser mealworm (*Alphitobius diaperinus*) protein concentrate produced by membrane emulsification: stability under simulated storage, process, and digestion conditions. *Foods* 10 (12). <https://doi.org/10.3390/foods10122997>.
- Wang, J., Jousse, M., Jayakumar, J., Fernández-Arteaga, A., de Lamo-Castellví, S., Ferrando, M., Güell, C., 2021b. Black soldier fly (*hermetia illucens*) protein concentrates as a sustainable source to stabilize O/W emulsions produced by a low-energy high-throughput emulsification technology. *Foods* 10 (5). <https://doi.org/10.3390/foods10051048>.
- Wang, J., Martínez-Hernández, A., de Lamo-Castellví, S., Romero, M.-P., Kaade, W., Ferrando, M., Güell, C., 2020. Low-energy membrane-based processes to concentrate and encapsulate polyphenols from carob pulp. *J. Food Eng.*, 109996 <https://doi.org/10.1016/j.jfoodeng.2020.109996>.